Local symmetry and magnetic anisotropy in multiferroic $MnWO_4$ and antiferromagnetic $CoWO_4$ studied by soft x-ray absorption spectroscopy

N. Hollmann,[1] Z. Hu,[1,2] T. Willers,[1] L. Bohatý,[3] P. Becker,[3] A. Tanaka,[4] H. H. Hsieh,[5] H.-J. Lin,[6] C. T. Chen,[6] and L. H. Tjeng[1,2]

[1]*II. Physikalisches Institut, Universität zu Köln, Zülpicher Str. 77, 50937 Köln, Germany*

[2]*Max Planck Institute for Chemical Physics of Solids, Nöthnitzerstr. 40, 01187 Dresden, Germany*

[3]*Institut für Kristallographie, Universität zu Köln, Zülpicher Str. 49b, 50674 Köln, Germany*

[4]*Department of Quantum Matter, ADSM, Hiroshima University, Higashi-Hiroshima 739-8530, Japan*

[5]*Chung Cheng Institute of Technology, National Defense University, Taoyuan 335, Taiwan*

[6]*National Synchrotron Radiation Research Center, 101 Hsin-Ann Road, Hsinchu 30077, Taiwan*

(Received 22 September 2010; published 23 November 2010)

Soft x-ray absorption experiments on the transition-metal $L_{2,3}$ edge of multiferroic $MnWO_4$ and antiferromagnetic $CoWO_4$ are presented. The observed linear polarization dependence, analyzed by full-multiplet calculations, is used to determine the ground-state wave function of the magnetic Mn^{2+} and Co^{2+} ions. The impact of the local structure and the spin-orbit coupling on the orbital moment is discussed in terms of the single-ion anisotropy. It is shown that the orbital moment in $CoWO_4$ is responsible for the collinear antiferromagnetism, while the small size of spin-orbit coupling effects make spiral magnetic order in $MnWO_4$ possible, enabling the material to be multiferroic.

DOI: 10.1103/PhysRevB.82.184429 PACS number(s): 71.20.Be, 78.70.Dm, 71.70.Ch, 75.30.Gw

I. INTRODUCTION

The combination of magnetic order and ferroelectricity in multiferroic compounds is a topic that has gained high interest in modern research.[1] Magnetic transitions directly linked to a spontaneous electrical polarization have been investigated in detail for materials such as $RMnO_3$ ($R=Y,Tb,Gd,Dy$) (Refs. 2–4) and $TbMn_2O_5$.[5] Among the multiferroic manganates, $MnWO_4$ takes a special place as it does not contain a rare-earth ion, leaving Mn formally as the only magnetic ion.[6,7]

Multiferrocity in these materials is explained by the spin-current model,[8,9] where the electrical polarization is caused by a spiral order of the magnetic moments. The spin-rotation axis **e** does not coincide with the magnetic propagation vector **Q**, leading to a nonvanishing spontaneous polarization $\mathbf{P} \propto \mathbf{e} \times \mathbf{Q}$. Here we investigate the conditions for the occurrence of spiral magnetic order responsible for the rich physics of $MnWO_4$. We performed soft x-ray absorption spectroscopy (XAS) on $MnWO_4$ to determine the local electronic and magnetic properties of the Mn ions. The results are also compared to measurements on the isostructural compound $CoWO_4$, which is a collinear antiferromagnet and not a multiferroic material. We analyze the role of the spin-orbit coupling and its impact on the magnetic structure. The magnitude of the single-ion anisotropy is calculated using the full-multiplet configuration-interaction approach. This forms the key to understand why in $MnWO_4$ spiral magnetic order is possible and why it is suppressed in $CoWO_4$.

II. EXPERIMENTAL

Single crystals of $MnWO_4$ and $CoWO_4$ were grown from the melt. During the single-crystal growth process of $MnWO_4$ special care was taken to keep manganese in divalent state. This was achieved by the use of high growth temperatures and the renouncement of melt solvents. Using the top seeded growth technique and low cooling rate (0.08 K/h), ruby-red transparent single crystals were obtained starting from a growth temperature of 1574 K.[10] Single crystals of $CoWO_4$ were obtained from $Na_2W_2O_7$ melt solution with a small surplus of WO_3 (molar ratio $CoWO_4$: $Na_2W_2O_7$: WO_3=1: 2: 0.5), starting at 1363 K and applying a cooling rate of 3 K/h. $MnWO_4$ and $CoWO_4$ belong to the monoclinic space group $P2/c$.

The XAS spectra were collected at the Dragon Beamline of the National Synchrotron Radiation Research Center in Hsinchu, Taiwan. The samples were cleaved *in situ* in an ultrahigh-vacuum chamber with pressures in the 10^{-10} mbar range, guaranteeing the high surface quality required to perform bulk-representative XAS studies in the total electron yield mode. The degree of linear polarization was $99 \pm 1\%$, with an energy resolution of approximately 0.3 eV. The linear polarization dependence was obtained by rotating the samples azimuthally around the Poynting vector of incoming light. This measurement geometry allows to measure different polarizations without changing the optical path, thus making a reliable comparison of the spectra possible. The spectra were collected at room temperature in the paramagnetic phase of both compounds. Single crystals of MnO and CoO were measured simultaneously in a separate chamber as references for $MnWO_4$ and $CoWO_4$, respectively.

III. SPECTROSCOPIC RESULTS

Figure 1 shows the room temperature Mn $L_{2,3}$ XAS spectra of $MnWO_4$ taken with the **E** vector of the light parallel to the **a**, **b**, and **c** crystallographic axes. The spectrum of a MnO single crystal is also included for reference purposes. The spectra are dominated by the Mn $2p$ core-hole spin-orbit coupling which splits the spectrum roughly in two parts, namely, the $L_3(h\nu \approx 638-645$ eV) and $L_2(h\nu$

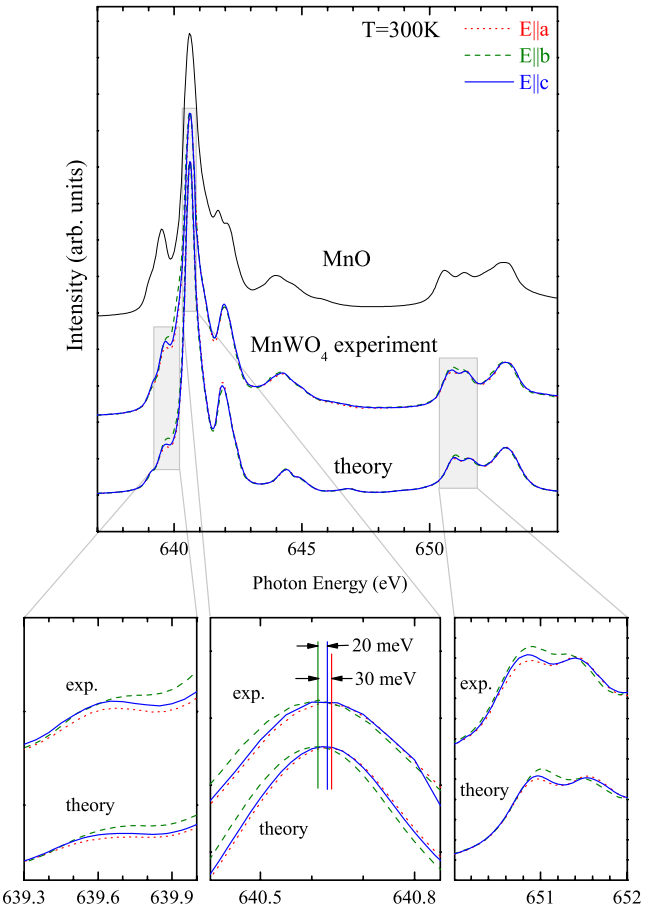

FIG. 1. (Color online) Top panel: experimental and theoretical Mn $L_{2,3}$ XAS spectra of $MnWO_4$ with the **E** vector of the light parallel to the **a**, **b**, and **c** crystallographic axes. The spectrum of MnO is included as reference. Bottom panels: a closeup revealing the polarization dependence of the spectra.

$\approx$649–654 eV) white line regions. The line shape strongly depends on the multiplet structure given by the Mn 3*d*-3*d* and 2*p*-3*d* Coulomb and exchange interactions, as well as by the local crystal fields and the hybridization with the O 2*p* ligands. Unique to soft XAS is that the dipole selection rules are very sensitive in determining which of the $2p^5 3d^{n+1}$ final states can be reached and with what intensity, starting from a particular $2p^6 3d^n$ initial state ($n=5$ for Mn^{2+}).[11,12] This makes the technique extremely sensitive to the symmetry of the initial state, i.e., the valence and the crystal-field states of the ions.

Comparing the $MnWO_4$ spectra with the MnO, one can immediately observe that the spectral features are similar with the L_3 main peaks at identical energies. This indicates directly that the Mn ions in $MnWO_4$ are also in the high-spin Mn^{2+} electronic configuration as the Mn ions in MnO. Yet, the clear differences between the spectra of $MnWO_4$ and MnO, as seen, e.g., at the low- and high-energy shoulders of the L_3 white line, provide a hint to a crystal-field level scheme different from O_h for the $MnWO_4$ system.

A small but clear polarization dependence for $MnWO_4$ was found, as can be seen in the bottom panels of Fig. 1, where a closeup is shown of the spectra taken with the three

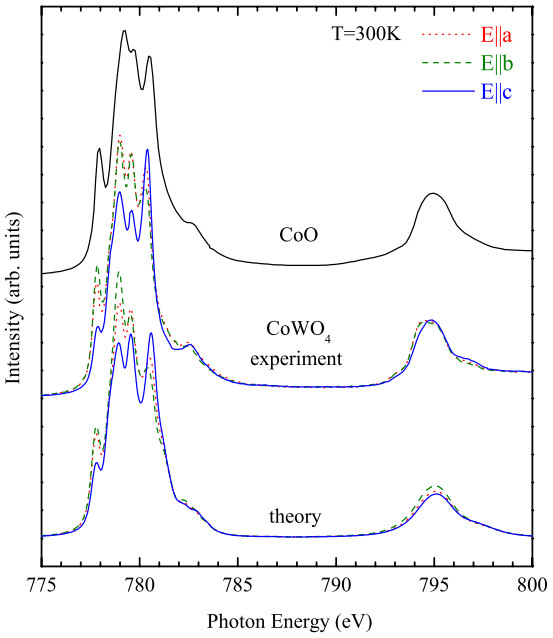

FIG. 2. (Color online) Experimental and theoretical Co $L_{2,3}$ XAS spectra of $CoWO_4$. The spectrum of multidomain CoO single crystal is included as reference.

different polarizations. The intensities as well as the energy positions of several peaks vary with the polarization of the incoming light. This polarization dependence is yet another indication that the local symmetry of the Mn ions in $MnWO_4$ is lower than O_h.

Figure 2 depicts the Co $L_{2,3}$ XAS spectra of $CoWO_4$ taken with the **E** vector of the light parallel to the **a**, **b**, and **c** crystallographic axes, together with the spectrum of a multidomain CoO single crystal as reference. Following the same argumentation as given above for the Mn $L_{2,3}$ edge, from the strong similarities between the $CoWO_4$ and the CoO spectra we can conclude that $CoWO_4$ contains Co^{2+} ions with a $3d^7$ high-spin configuration like in CoO. In comparing the $CoWO_4$ with the $MnWO_4$, one observes that the polarization dependence is much larger. In the following we will discuss the different origins of the linear polarization dependence for the two compounds and its implications for their very different magnetic properties.

IV. LOCAL ELECTRONIC STRUCTURE

To interpret and understand the spectral line shapes and their polarization dependence, we have performed simulations of the atomiclike $2p^6 3d^n \rightarrow 2p^5 3d^{n+1}$ ($n=5$ for Mn^{2+} and $n=7$ for Co^{2+}) transitions using the well-proven configuration-interaction cluster model.[11–13] Within this method we have treated the Mn or Co ion within an MnO_6 or CoO_6 cluster, respectively, which includes the full atomic multiplet theory and the local effects of the solid. It accounts for the intra-atomic 3*d*-3*d* and 2*p*-3*d* Coulomb interactions, the atomic 2*p* and 3*d* spin-orbit couplings, the local crystal field, and the O 2*p*-Mn 3*d* or O 2*p*-Co 3*d* hybridization. This hybridization is taken into account by adding the $3d^{n+1}\underline{L}$

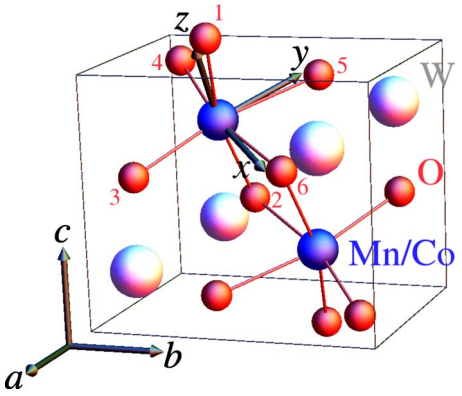

FIG. 3. (Color online) The structure of $MnWO_4$ and $CoWO_4$. For the calculations of the XAS spectra, a local coordinate system (x,y,z) was introduced, in which the axes point roughly along the Mn/Co-O bonds. The global crystallographic coordinates system can be transformed into the local coordinate system by rotating along b by ≈34° and then along the c axis by 45° (see text for more details).

and $3d^{n+2}\underline{L}^2$, etc., states to the starting $3d^n$ configuration, where $\underline{L}$ denotes a hole in the O p ligands.

To facilitate the setup and the interpretation of the calculations, a local coordinate system was introduced, with its axes (x,y,z) pointing roughly along the Mn-O and Co-O bonds. To transform the global coordinates (a,b,c) into the local system, first a rotation by 33.9° along b is applied, resulting in a new system with (a',b',c'). This system is then rotated by 45° along the *old* axis c, transforming (a',b',c') into (x,y,z). The local coordinate system is shown in Fig. 3. The coordinates of the oxygen ions as well as the Mn-O and Co-O distances are summarized in Table I. The crystal structure has been taken from Ref. 14. There are two distorted octahedra in the unit cell and they are connected to each other by inversion, thereby contributing to the polarization dependence in the same manner.

The Mn-O and Co-O bond lengths were used to estimate the hybridization strength using Harrison's description,[15] resulting in values for $pd\sigma$ and $pd\pi$ as shown in Table I. The Slater-Koster formalism[16] provides the angular dependence of the hybridization strength. Values for the crystal fields were tuned to find the best match to the experimental spectra. Parameters for the multipole part of the Coulomb interactions were given by the Hartree-Fock values[12] while the monopole parts (U_{dd},U_{pd}) were estimated from photoemission experiments on MnO (Ref. 17) and previous work on CoO.[18] The simulations were carried out using the program XTLS 8.3,[12] and the parameters used are listed in Refs. 19 and 20.

The calculated polarization-dependent spectra for the Mn $L_{2,3}$ edge of $MnWO_4$ are plotted in Fig. 1. One can observe that the general line shape of the experimental spectra is very well reproduced. Equally important, also the small energy shifts in the peak positions as well as the small variations in the peak intensities as a function of polarization can all be simulated. This indicates that we have been able to capture the local electronic structure of the Mn ion in $MnWO_4$ with great accuracy. We now will look into this in more detail.

The ground state of a Mn^{2+} ion in O_h symmetry is $^6A_1$, and this will not split or change upon lowering the crystal symmetry.[21,22] The electronic charge distribution of this high-spin half-filled shell ion remains spherical. The presence of lower symmetry crystal fields will then show up most clearly when an electron is added (or removed) from the valence shell. To illustrate such a situation, we depict in

TABLE I. Coordination of the Mn^{2+} and Co^{2+} ions in their distorted oxygen octahedra. All oxygen positions are given in angstrom in the local coordinate system specified in Fig. 3, where the numbering of the atoms is also defined. The hybridization strengths $pd\sigma$ and $pd\pi$ are in units of electron volt.

$MnWO_4$						
O	x	y	z	Mn-O dist.	$pd\sigma$	$pd\pi$
1	0.25	0.24	2.15	2.18	−1.18	0.54
2	0.25	0.24	−2.15	2.18	−1.18	0.54
3	0.31	−2.07	−0.02	2.09	−1.36	0.63
4	−2.06	0.36	0.02	2.09	−1.36	0.63
5	0.31	2.24	−0.08	2.27	−1.02	0.47
6	2.25	0.25	0.08	2.27	−1.02	0.47
$CoWO_4$						
O	x	y	z	Co-O dist.	$pd\sigma$	$pd\pi$
1	0.19	0.19	2.10	2.12	−1.07	0.49
2	0.19	0.19	−2.10	2.12	−1.07	0.49
3	0.24	−2.02	−0.04	2.03	−1.24	0.57
4	−2.02	0.25	0.04	2.03	−1.24	0.57
5	0.24	2.14	−0.03	2.16	−1.01	0.47
6	2.14	0.23	0.03	2.16	−1.01	0.47

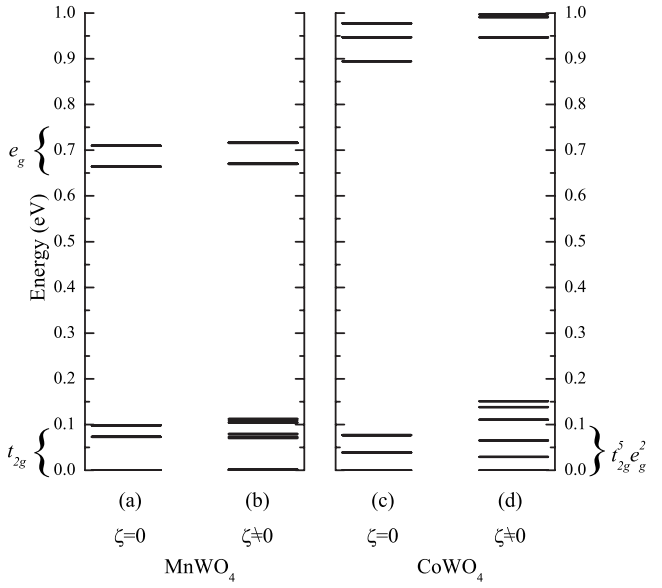

FIG. 4. Energy-level diagrams for (a) and (b) Mn^+ ($3d^6$) and (c) and (d) Co^{2+} clusters, excluding and including the $3d$ spin-orbit coupling ζ. Only the states up to 1 eV are shown.

the left panel of Fig. 4 the total energy-level diagram of a Mn^+ ($3d^6$) ion using the crystal and ligand field parameters which reproduce best the Mn $L_{2,3}$ spectra of $MnWO_4$ as described above. One can readily observe a splitting of about 0.7 eV between states with the added electron in the t_{2g} vs the e_g orbitals. Upon switching off the $3d$ spin-orbit interaction, see Fig. 4(a), one can also identify an intra-t_{2g} splitting of about 65 and 95 meV as well as an intra-e_g splitting of 50 meV. All of the orbitals are of mixed type as a result of the low local symmetry. The two orbitals lowest in energy are approximately $1/\sqrt{2}(xz+yz)$ and $1/\sqrt{2}(xz-yz)$, resembling the xz and yz orbitals, rotated by $\pm 45°$ along z. This is a result of the local S_2 symmetry axis of the MnO_6 cluster, which lies in the xy plane with an angle of roughly 45° to the oxygen bonds.

Also in the Mn $L_{2,3}$ XAS process one extra electron is added into the valence shell. The lowest-lying peak at 639.6 eV, see Fig. 1, involves the excitation of the $2p$ core electron into the t_{2g} orbitals. Different polarizations access different orbitals with different probabilities. For the 640.6 eV peak, the polarization dependence is reflected in terms of shifts in its energy position. If one could have measured the polarization dependence along the local coordinates of one Mn ion, one may expect to observe peak shifts of 65 and 95 meV associated with the intra-t_{2g} splittings shown in Fig. 4. Yet, having two Mn ions in the unit cell, and measuring along the global a, b, and c crystallographic directions, the shifts between the effectively composite peaks become reduced. In the experiments and in the simulations we are left with shifts of about 20 and 30 meV as can be seen in the middle bottom panel of Fig. 1. For the 639.6 eV peak, the shifts due to variation in the polarization are more difficult to quantify since there is also a variation in the intensity of the peaks. The latter is apparently caused by the rather complicated multiplet effects involving the $2p$ core hole, as demonstrated by the excellence of the match by the simulations, see the left bottom panel of Fig. 1. These intensity variations are yet quite small, and *integrated* over the entire $L_{2,3}$ range, would have been even identical to zero if the noncubic hybridization effects were absent.

The simulations for the polarization dependent spectra for the Co $L_{2,3}$ edge of $CoWO_4$ are shown in Fig. 2. Like in the Mn case, we have been able to achieve a satisfying fit to the experimental spectra: all features are well reproduced, including the strong polarization dependence. We will now analyze the local electronic structure of the Co ion on the basis of the parameters used in these simulations.

For the Co^{2+} ions, the ground state of the $3d^7$ configuration in O_h symmetry is ${}^4T_1$ ($\approx t_{2g}^5 e_g^2$). Unlike for the ${}^6A_1$ of the Mn, this ${}^4T_1$ state will be split upon going to lower crystal symmetry. The degeneracy in the orbital part, i.e., in the t_{2g} subshell, will be lifted. This can be seen from the total energy-level diagram shown in the right panel of Fig. 4. The calculation with the $3d$ spin-orbit interaction switched off, see Fig. 4(c), reveals the presence of three low-lying quartets within the first 0.1 eV. In an one-electron language, each of them would correspond to the hole occupying one of the three t_{2g} orbitals. The intra-t_{2g} splittings are 40 and 80 meV. These values are quite close to those of the $MnWO_4$ case reflecting the similar crystal structure. The importance of the lifted degeneracy is that the orbital occupation will no longer be isotropic, i.e., the Co-ion charge distribution will be highly nonspherical. This then explains the strong polarization dependence in the absorption spectra.

It is also important to notice how the low-lying states of Co^{2+} are influenced by the $3d$ spin-orbit coupling. The energy level diagram in Fig. 4(d) reveals that there is indeed a large amount of mixing due to spin-orbit interaction. The spin-orbit coupling constant of $\zeta=66$ meV is of the same order of magnitude as the splittings in the t_{2g} subshell. All this has direct consequences on the magnetism, as will be discussed in the next section.

V. SINGLE-ION ANISOTROPY

From the results of the simulation, we find that the $3d$ spin-orbit interaction has a major influence on the energies and nature of the low-lying states of the $CoWO_4$ system. The magnetic moment will then not only have a spin contribution but also an appreciable orbital one. This results in a strong coupling of the direction of magnetic moment to the crystal structure. We can make an estimate of the single-ion anisotropy of the Co^{2+} ion. For that we use the same parameters with which we have reproduced the XAS spectra and the polarization dependence therein, and we apply a small exchange field of $\mu_B H_{ex}=10^{-6}$ eV ($H_{ex}\approx 200$ Oe) to align the magnetic moment. Here we would like to note that the results hardly change with increasing the strength of the field, i.e., they are robust even beyond $\mu_B H_{ex}=10^{-2}$ eV.

Figure 5 shows the expectation value of the magnetization parallel to the applied exchange field $M_{\parallel}$ as a three-dimensional representation and in a polar plot, the latter in local coordinates. It can be seen that the single-ion anisotropy is of easy-axis type, with the axis lying along $\phi=135°$ at $\theta=90°$ in the local coordinate system. In the direc-

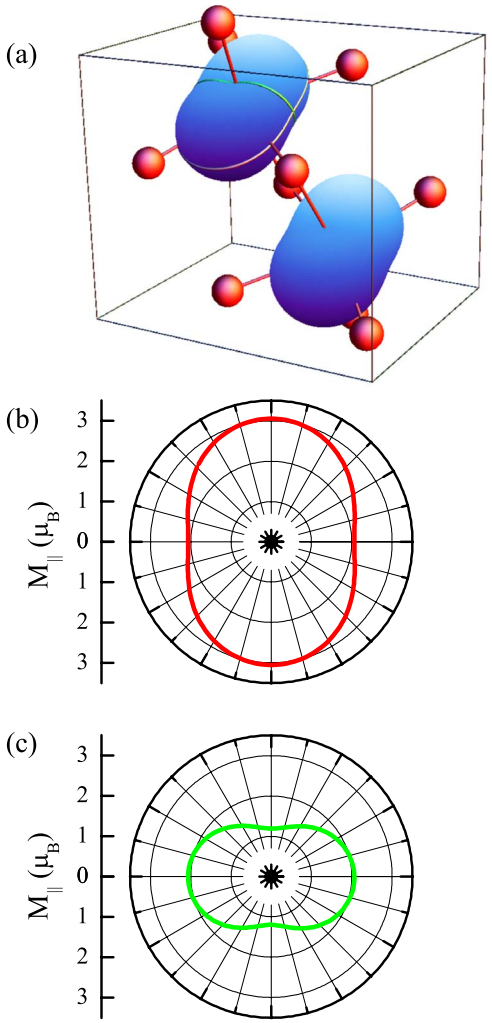

FIG. 5. (Color online) Calculated magnetic anisotropy of Co^{2+} in $CoWO_4$. (a) Three-dimensional representation of the magnetic anisotropy in the unit cell. The surface depicts the expectation value of the magnetic moment $M_{\parallel}$ pointing parallel to a small exchange field applied to the ion. (b) Two-dimensional cut of $M_{\parallel}$ in the plane of easy and intermediate magnetic axis (corresponding approximately to the *xy* plane in local coordinates). (c) Cut through the plane of hard and intermediate magnetic axis.

tion of the easy axis, the moment is completely directed along the magnetic field, and the perpendicular component of the magnetization vanishes. The easy axis is also perpendicular to the S_2 symmetry axis of the distorted octahedron, reflecting the orbital character of the two lower-lying ligand field levels. The total magnetic moments of the hard and easy axes are 1.2 μ_B and 3.0 μ_B, respectively, with an orbital contribution of 0.1 μ_B and 0.9 μ_B. The easy axis of the total moment coincides directly with that of the orbital moment, which is also pointed out earlier by Bruno.[23] It has also been reported that for low symmetries, the orbital and total moment could differ in their behavior due to the magnetic dipole moment T_z.[24] In the case of $CoWO_4$, however, with the symmetry of the CoO_6 groups being not too far from cubic, this T_z is around −0.01 eV, and does not influence the anisotropy significantly.

In $CoWO_4$, the single-ion anisotropy is strong enough to lead to an effective pinning of the spins in the magnetically ordered phase. Isotropic superexchange will be the dominating magnetic interaction, although in addition anisotropic exchange is possible, as the bonds lack inversion centers. But the Dzyaloshinskii-Moriya (DM) term $\mathbf{D}\cdot(\mathbf{S}_1\times\mathbf{S}_2)$, that favors canted magnetic moments, is small compared to the energy involved in the magnetic anisotropy of $CoWO_4$, reflected by the large difference in moment of more than 1 μ_B. The superexchange will then minimize the energy in the magnetically ordered phase by aligning the moments along the easy axis. The easy axis is identical for both CoO_6 clusters in the unit cell, and thus the single-ion anisotropy itself will not lead to canting between the magnetic moments of the Co^{2+} ions. The result is a collinear antiferromagnet with an easy axis approximately in the *ac* plane ≈40° off from *a*. This direction is illustrated in Fig. 5 and is close to the one found in the experiment by neutron diffraction.[25]

Returning to $MnWO_4$ case: to the leading order, the local spherical $^6A_1$ ground state does not produce an orbital moment. The spin is then free to point in any direction. This is reproduced in the calculation, where the response of the magnetic moment to an exchange field is practically isotropic. Yet, in second order, the spin-orbit coupling does affect the Mn-O hopping. This produces a nonvanishing moment perpendicular to the exchange field, albeit in the order of 10^{-2} μ_B, being much lower than in the case of the spin-orbit active $CoWO_4$. Consequently, the DM term is on the same energy scale as the anisotropy, and spin canting can easily occur. The propagation direction of the spiral magnetic order is in the *local xy* plane, meaning that the second order process leads to a hard axis along *z*. This demonstrates the importance of the single-ion anisotropy in this system. The form of the anisotropy, however, depends strongly on the magnetic exchange. This explains that even three different magnetically ordered phases exist in the material at low temperatures.[26] Additionally to the hard axis, the easy plane also has two principal axes for the magnetic anisotropy with a small difference between the two. This, in combination with the subtle dependency of the anisotropy on the exchange field, makes incommensurabilities likely to appear.

VI. CONCLUSION

The single-ion anisotropies extracted from our soft x-ray absorption data and the corresponding full-multiplet calculations provide a natural explanation for the magnetic ordering phenomena occurring in $CoWO_4$ and $MnWO_4$. In $CoWO_4$, the spin-orbit coupling and a nonvanishing orbital moment overwhelm the anisotropic Dzyaloshinskii-Moriya exchange and cause the formation of a collinear ordering of the moments. Contrary to that, although being isostructural, $MnWO_4$ shows only a small magnetic anisotropy which is comparable in energy to the Dzyaloshinskii-Moriya interactions. This will cant the spins in such a way that the spiral propagates perpendicular to the direction of smallest magnetic moment, allowing a modulated spin spiral which causes the ferroelectricity in the material.

ACKNOWLEDGMENTS

We gratefully acknowledge the NSRRC staff for providing us with beamtime. The research in Cologne is supported by the Deutsche Forschungsgemeinschaft through SFB 608. N.H. is also supported by the Bonn-Cologne Graduate School of Physics and Astronomy. We are grateful for discussions with M. W. Haverkort and D. I. Khomskii.

[1] M. Fiebig, J. Phys. D **38**, R123 (2005).
[2] M. Fiebig, T. Lottermoser, D. Frohlich, A. V. Goltsev, and R. V. Pisarev, Nature (London) **419**, 818 (2002).
[3] T. Kimura, T. Goto, H. Shintani, K. Ishizaka, T. Arima, and Y. Tokura, Nature (London) **426**, 55 (2003).
[4] T. Goto, T. Kimura, G. Lawes, A. P. Ramirez, and Y. Tokura, Phys. Rev. Lett. **92**, 257201 (2004).
[5] N. Hur, S. Park, P. A. Sharma, J. S. Ahn, S. Guha, and S. W. Cheong, Nature (London) **429**, 392 (2004).
[6] O. Heyer, N. Hollmann, I. Klassen, S. Jodlauk, L. Bohaty, P. Becker, J. A. Mydosh, T. Lorenz, and D. Khomskii, J. Phys.: Condens. Matter **18**, L471 (2006).
[7] K. Taniguchi, N. Abe, T. Takenobu, Y. Iwasa, and T. Arima, Phys. Rev. Lett. **97**, 097203 (2006).
[8] H. Katsura, N. Nagaosa, and A. V. Balatsky, Phys. Rev. Lett. **95**, 057205 (2005).
[9] M. Mostovoy, Phys. Rev. Lett. **96**, 067601 (2006).
[10] P. Becker, L. Bohatý, H. J. Eichler, H. Rhee, and A. A. Kaminskii, Laser Phys. Lett. **4**, 884 (2007).
[11] F. M. F. de Groot, J. Electron Spectrosc. Relat. Phenom. **67**, 529 (1994).
[12] A. Tanaka and T. Jo, J. Phys. Soc. Jpn. **63**, 2788 (1994).
[13] G. van der Laan, J. Electron Spectrosc. Relat. Phenom. **86**, 1 (1997).
[14] G. Lautenschläger, H. Weitzel, T. Vogt, R. Hock, A. Böhm, M. Bonnet, and H. Fuess, Phys. Rev. B **48**, 6087 (1993).
[15] W. A. Harrison, *Electronic Structure and the Properties of Solids* (Dover, New York, 1989).
[16] J. C. Slater and G. F. Koster, Phys. Rev. **94**, 1498 (1954).
[17] A. E. Bocquet, T. Mizokawa, T. Saitoh, H. Namatame, and A. Fujimori, Phys. Rev. B **46**, 3771 (1992).
[18] S. I. Csiszar, M. W. Haverkort, Z. Hu, A. Tanaka, H. H. Hsieh, H.-J. Lin, C. T. Chen, T. Hibma, and L. H. Tjeng, Phys. Rev. Lett. **95**, 187205 (2005).
[19] MnO_6 cluster parameters (eV): Δ=6.5, U_{dd}=7.0, U_{pd}=8.0, Slater integrals reduced to 85% of Hartree-Fock values.
[20] CoO_6 cluster parameters (eV): Δ=6.5, U_{dd}=6.5, U_{pd}=8.2, Slater integrals reduced to 80% of Hartree-Fock values.
[21] C. J. Ballhausen, *Introduction to Ligand Field Theory* (McGraw-Hill, New York, 1962).
[22] S. Sugano, Y. Tanabe, and H. Kamimura, *Multiplets of Transition-Metal Ions in Crystals* (Academic, New York, 1970).
[23] P. Bruno, Phys. Rev. B **39**, 865 (1989).
[24] G. van der Laan, J. Phys.: Condens. Matter **10**, 3239 (1998).
[25] H. Weitzel and H. Langhof, J. Magn. Magn. Mater. **4**, 265 (1977).
[26] H. Ehrenberg, H. Weitzel, C. Heid, H. Fuess, G. Wltschek, T. Kroener, J. van Tol, and M. Bonnet, J. Phys.: Condens. Matter **9**, 3189 (1997).